ELSEVIER

Nuclear Instruments and Methods in Physics Research B 193 (2002) 508–515

NIM B
Beam Interactions with Materials & Atoms

www.elsevier.com/locate/nimb

Large-angle back-scattering of Ar^{q+} ($q = 1$–13) during quasi-binary collisions with CsI(1 0 0) in the energy range 10 eV/q –2.8 keV/q: Energy loss analysis and scattered charge state distributions

F.W. Meyer [a,*], V.A. Morozov [a], J. Mrogenda [b], C.R. Vane [a], S. Datz [a,1]

[a] *Physics Division, Oak Ridge National Laboratory, MS-6372 Bldg. 6003, P.O. Box 2008, Oak Ridge, TN 37831-6372, USA*
[b] *Institut für Kernphysik, Universität Münster, D-48149 Münster, Germany*

Abstract

We report on measurements of absolute scattered projectile charge fractions for Ar^{11+} ions with incident energies in the range 3–30 keV, that have been 120° back-scattered from CsI(1 0 0) in quasi-binary collisions. Use of a time-of-flight technique that incorporates a biased drift region permitted full separation of all scattered charged states, including neutrals. In contrast to our Ar^{11+} results for Au(1 1 0), the scattered neutral fraction is smaller, and relatively independent of incident projectile energy over the entire investigated range. In addition, we have measured, at a fixed energy of ~5 keV, scattered charged state distributions as function of incident charge states in the range 1+ to 13+. In a separate measurement utilizing electrostatic instead of TOF analysis of the scattered charge states, we attempted to evaluate the effect of surface charging on energy loss of low energy scattered projectiles by absolute measurements of the scattered 1+ energies of incident Ar^{11+} ions incident on CsI(1 0 0) at energies down to 10 eV/q. Apart from small deviations from the elastic binary collision energy loss expected for large angle scattering, ascribable to the image charge interaction, no measurable effect due to surface charging was found down to the lowest investigated energies. © 2002 Elsevier Science B.V. All rights reserved.

PACS: 79.20.Rf; 79.20.Ap; 34.50.Dy; 61.18.Bn
Keywords: Ion–surface scattering; Highly charged projectile neutralization; CsI; Multicharged ions; Scattered charge state distributions

1. Introduction

In this contribution we investigate the incident charge state, incident energy, and energy loss dependence of projectile neutralization in large-angle back-scattering collisions of multicharged Ar ions from CsI(1 0 0). The motivation for this work arose in part from our previous measurements of scattered charge fractions for Ar^{q+} ions incident on Au(1 1 0) [1], which found significant energy dependence of the scattered neutral fractions as function of increasing energy, and the work of Briand et al. [2], which had identified significant signatures of surface charging in back-scattering of

* Corresponding author. Tel.: +1-1-865-574-4705; fax: +1-1-865-574-1118.
E-mail address: meyerfw@ornl.gov (F.W. Meyer).
[1] In Memoriam.

0168-583X/02/$ - see front matter © 2002 Elsevier Science B.V. All rights reserved.
PII: S0168-583X(02)00829-7

very low energy, highly charged Ar projectiles from Si–H. The intent of the present (as well as our previous [1,3,4] investigations) was to restrict the interaction to quasi-binary, well-defined large-scattering-angle binary collisions, thereby reducing the interaction times sufficiently to permit study of the scattered charge states prior to equilibration, both in terms of their energy loss and their dependence on incident projectile charge state and energy.

2. Experimental approach

The measurements were carried out at the ORNL Multicharged Ion Research Facility [5]. Fig. 1 shows a schematic diagram of the previously described experimental apparatus [6,7], which consists of an ultra-high vacuum (10^{-10} mbar) floating scattering chamber, a time-of-flight (TOF) analyzer with floatable drift tube, and a hemispherical sector electrostatic analyzer. The electrostatic analyzer was set for the present measurements at 136° and had a resolution of about 1.5%, while the TOF analyzer was fixed at an observation angle of 120°. The target was attached to a sample mount with two rotational degrees of freedom and was prepared by cycles of sputter cleaning under grazing incidence with 2 keV Ar^+ ions and successive annealing cycles at about 450 °C. The chopped primary beams of argon multicharged ions were decelerated from $(10 \times q)$ keV to the desired final energy in the range 0.1–33 keV before impacting the CsI(1 0 0) surface at normal incidence. To prevent macroscopic sample charging, the CsI(1 0 0) target was heated to a constant temperature of 250 °C during the measurements shown below.

Fig. 2 shows scattered projectile spectra obtained at an incident energy of about 2 keV. In Fig. 2(a) a typical TOF spectrum is displayed for incident Ar^{9+} at this energy. The spectrum exhibits rather sharp peaks originating from elastic binary collisions between the incident projectile and individual target atoms. Since these peaks, at least in the case of the Au(1 1 0) measurements, were found to include, for certain target azimuthal orientations, out-of-plane "hard–soft" double collisions having energy losses experimentally indistinguishable from true binary collisions, we refer

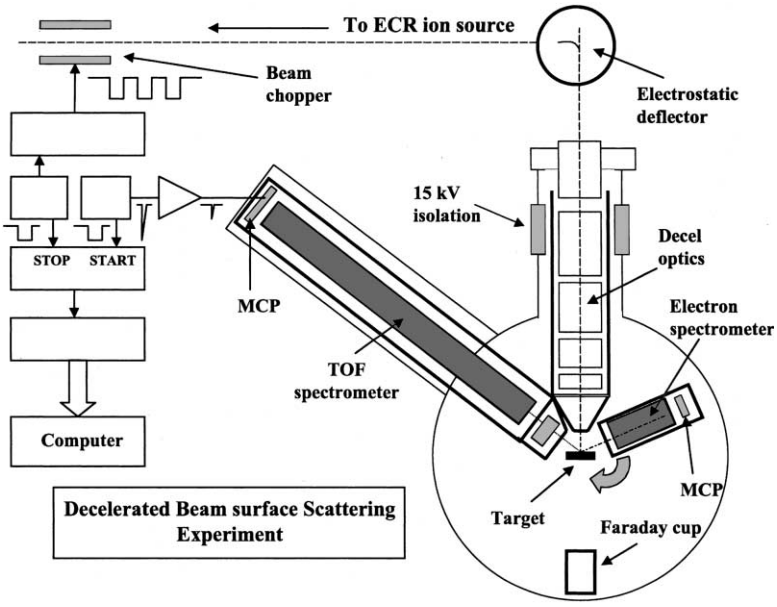

Fig. 1. Schematic diagram of the experimental apparatus, showing TOF spectrometer and associated electronics, electrostatic hemispherical sector analyzer (electron spectrometer in figure) and deceleration system.

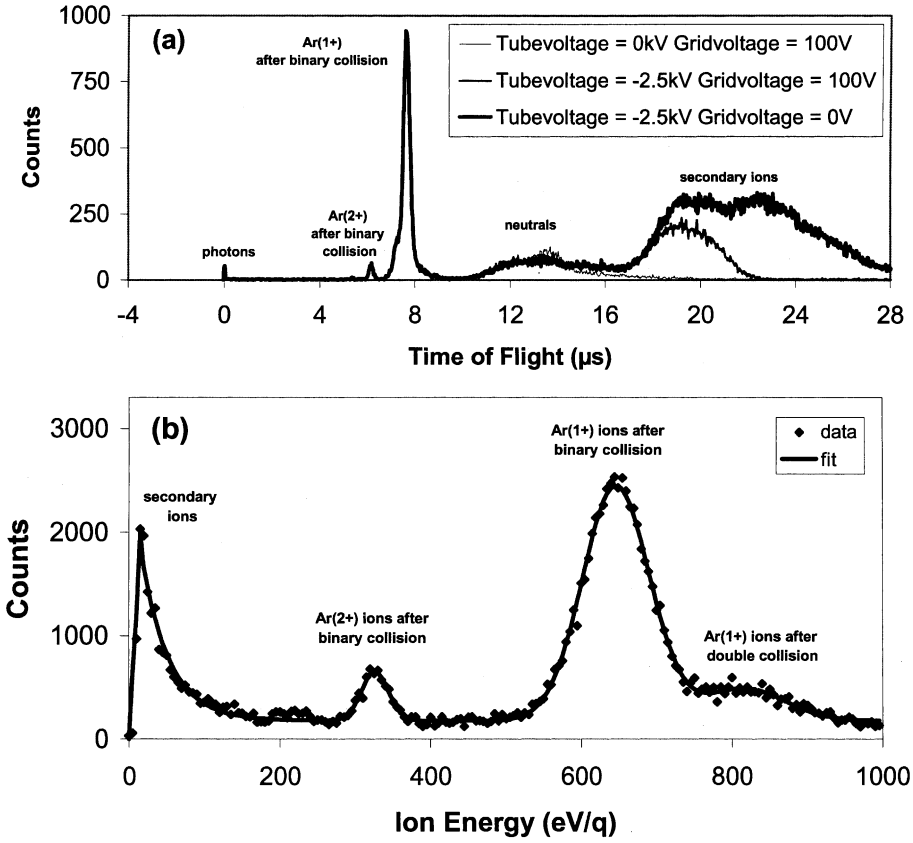

Fig. 2. Sample low-energy-impact scattered-projectile and secondary-ion energy distributions; (a) TOF spectra for 1.6 keV Ar^{9+} normally incident on CsI(1 0 0) for three different tube voltage/grid bias combinations (see text); (b) back-scattered energy spectrum for 2.04 keV Ar^{11+} incident on CsI(1 0 0) obtained with electrostatic analyzer – 136° observation angle.

to these peaks as quasi-binary [3]. A general feature of all the measured TOF spectra obtained with the CsI target is a prominent secondary ion component (identified in the figure), in addition to the features related to the scattered projectiles. This feature was not observed for a Au(1 1 0), and is ascribed to defect-mediated desorption [8] and/or kinetically assisted potential sputtering [9], as already observed and described for other alkali halide targets. The low energy tail of the secondary ions could be truncated by applying a positive bias voltage to the entrance grid to the TOF analyzer, as is also illustrated in the figure. Observation of these secondary ions was only possible with the flight tube and multichannel plate detector biased at negative high voltage, i.e. in the mode required for charge dispersion of the scattered projectiles, since without such acceleration their detection efficiency was effectively zero (note disappearance of secondary ions for zero tube voltage in the figure). Also to be noted is the apparent low intensity of scattered neutrals (both quasi-binary and those originating from multiple collisions) at the energy shown. This is part due to the non 100% detection efficiency for the scattered neutrals at energies much below 1 keV (which is corrected for as part of the charge fraction analysis), and in part due to the less efficient neutralization observed for CsI(1 0 0). This latter issue will be discussed in greater detail in a later section.

In Fig. 2(b), a scattered projectile energy spectrum is shown for 2 keV normally incident Ar^{11+},

obtained using the electrostatic spherical sector analyzer. The secondary peak to the right of the main binary collision back-scattered Ar^+ peak (less discernible in Fig. 2(a)) arises from true double collision back-scattering events analogous to what has been discussed by Huang et al. [10] for Au(1 1 1). The secondary ions already noted in connection with Fig. 2(a) now appear at their true energies (peaking at a few tens of eV for this incident projectile energy), since, in contrast to the TOF measurements, their acceleration to energies required for efficient detection occurred subsequent to their energy analysis, i.e. just prior to impact on the multichannel plate. The electrostatic analysis method proved to be most convenient for the low energy back-scattering measurements intended to probe the effects of surface charging, since the ion beams could be used unchopped, meaning a factor of 1000 higher beam intensities, and were also free of chopping-related energy shifts, which would have required additional corrections. The TOF approach, on the other hand, was employed for the higher energy measurements, since they would have required analyzing voltages beyond the physical limits of the electrostatic analyzer and the power supplies used.

To illustrate the increased complexity of the TOF spectra at higher energies, Fig. 3 shows typical scattered projectile TOF spectra for an Ar^{11+} projectile incident normally on CsI(1 0 0) at 15 keV. In comparison to the TOF spectra obtained with Au(1 1 0), the quasi-binary collision peaks are broader, consisting of unresolved contributions from Cs and I scattering centers. Second, in contrast to the Au(1 1 0) results, where multiple collisions formed a background mainly for scattered neutrals, a significant multiple collision background is evident for the scattered 1+ charge states as well in the case of CsI(1 0 0), creating additional "background". These two facts, combined with a quasi-binary neutral peak that is less clearly resolved from the broad multiple collision base upon which it sits, complicated background stripping, particularly at the higher incident energies, where the separation of adjacent scattered charge states was limited by the maximum attainable drift tube voltage of −4 kV. Some background subtraction was accomplished by taking differences between

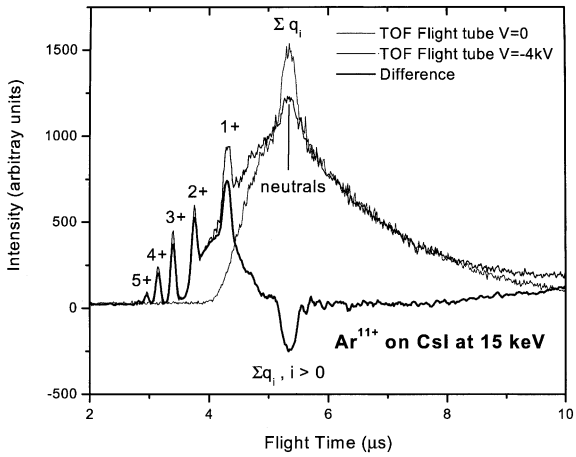

Fig. 3. TOF spectra for Ar^{11+} normally incident on CsI(1 0 0) with flight tube at high voltage, and at ground potential; the difference spectrum also shown was used to eliminate large part of multiple collision neutral background, as well as to determine the detection efficiency at a given energy (see [6]).

spectra obtained with the flight tube at negative high voltage and with it grounded, examples of both being shown in the figure. The final step of determining peak areas was accomplished by use of multi-Gaussian, non-linear fitting routines. As has already been discussed in greater detail elsewhere [7], the final peak areas were all corrected for differences in collection and detection efficiencies resulting from the charge-state-dependent focusing of the scattered ions upon entry into the floating drift tube section of the TOF analyzer, and the charge-dependent impact-energies on the multichannel plate detector, respectively.

As was the case for the Au(1 1 0) target, both the shape and intensity of the multiple collision background, and to a smaller extent, the intensities of quasi-binary collision peaks, were found to be functions of incidence angle and target azimuth orientation. In the absence of a more detailed simulation analysis similar to that performed in connection with our Au(1 1 0) measurements, close to normal incidence conditions were used, where, given the simple cubic lattice structure and the [1 0 0] target surface used, shadowing and blocking were expected to minimize interactions with all but the top two layers.

3. Results

Fig. 4(a) shows results for the peak energies of quasi-binary-collision-scattered Ar^{+} and Ar^{2+}, as well as of true-double-collision-scattered Ar^{+} ions as function of incident Ar projectile energy, for an incident projectile charge state of 11+. The solid and dashed straight lines in the figure show the expected dependences on incident projectile energy for binary scattering from Cs and I scattering sites, respectively. Fig. 4(b) shows the ratio of Ar^{2+}/Ar^{+} peak areas as well as the corresponding ratio for secondary ions as function of incident Ar energy. Goal of these low energy scattering measurements was to obtain evidence for the so-called "trampoline" effect described by Briand et al. [2], in the form of an increase of the effective mass of the target collision partner, as the projectile is back-scattered from a charge cloud encompassing many scattering centers, instead of a single lattice site, which should manifest itself as a significant deviation from the linear relationship between scattered and incident projectile energies expected for binary collisions, and in the form of an increasing 2+/1+ ratio, as the collision turning point moves progressively further away from the surface with decreasing energy, resulting in progressively higher survival fractions of the higher charge states (as also seen by Briand et al. [2]). Anticipating our discussion in a later section, neither of these characteristics are in fact manifested in the present measurements.

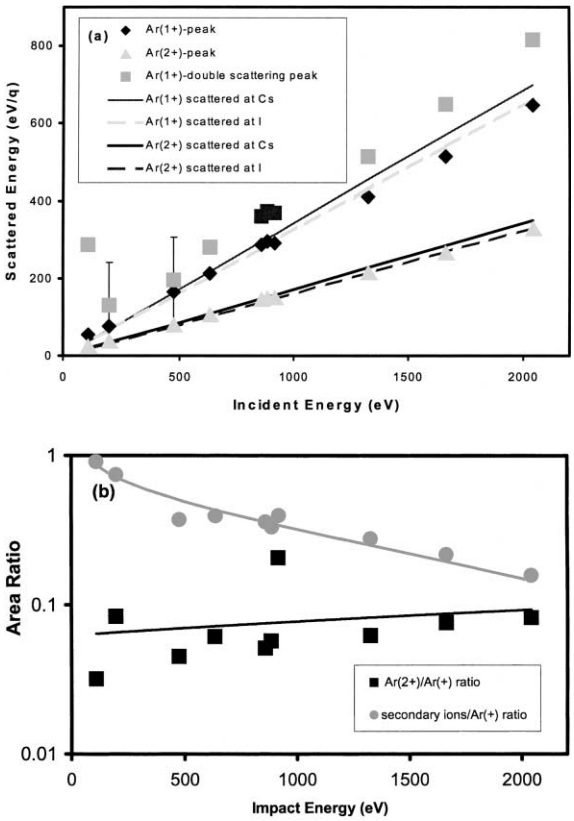

Fig. 4. (a) Plot showing final energies of Ar^{+} back-scattered 136° from CsI(1 0 0) in single and double collisions, and of single collision back-scattered Ar^{2+} as function of incident Ar^{11+} projectile energy; the solid and dashed lines represent the final energies/charge of Ar^{+} and Ar^{2+} projectiles expected after 136° back-scattering in a binary collision from Cs and I lattice sites, respectively; (b) Ar^{2+}/Ar^{+} peak area ratios, as well as the ratio of secondary ions/Ar^{+} peak areas, as function of incident Ar^{11+} energy – lines through the data are to guide the eye.

Turning now to our higher energy TOF results for CsI(1 0 0), two sets of measurements were carried out, in analogy to our previous measurements with Au(1 1 0) [1]. Fig. 5 summarizes scattered charge fractions determined at a fixed incidence energy of 5 keV as function of incident projectile charge state, in the range 1+ to 13+. Fig. 6 shows the energy dependence of scattered

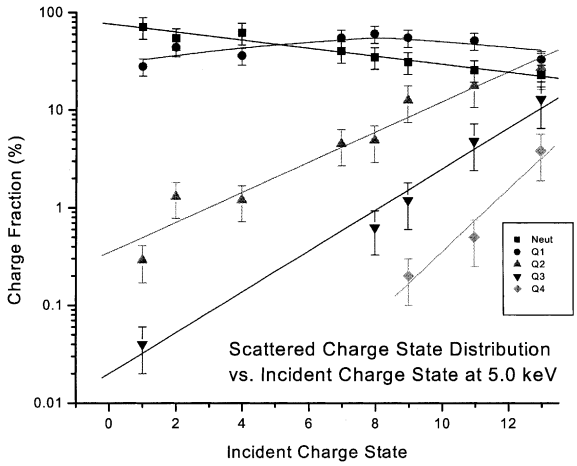

Fig. 5. Scattered charge fractions for 120° back-scattered Ar^{q+} ($q = 1$–13) projectiles normally incident on CsI(1 0 0) at 5 keV; lines through data points are meant only to guide the eye.

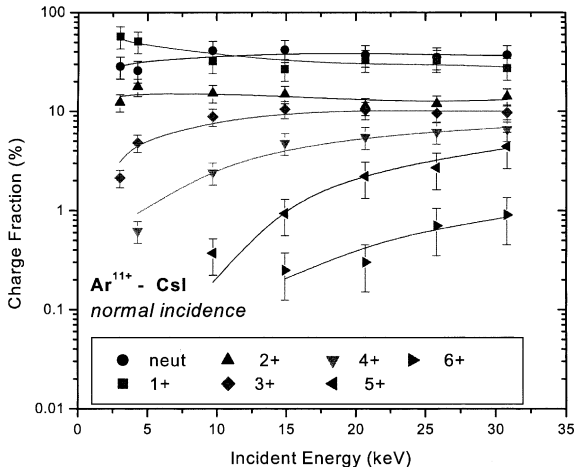

Fig. 6. Scattered charge fractions for 120° back-scattered Ar^{11+} projectiles normally incident on CsI(1 0 0) as function of incident energy; lines through data points are meant only to guide the eye.

charge fractions for a fixed incident charge state, 11+, in the energy range 3–32 keV. All measurements were obtained under normal incidence conditions and fixed target azimuth.

4. Discussion

4.1. Low energy scattered energy and area ratio results

As a very low-energy projectile approaches an insulator surface, a number of competing processes can occur. The projectile image charge interaction (whose magnitude depends on the dielectric response of the target) results in acceleration toward the surface. Electrons emitted toward the approaching projectile leave behind positive holes whose repulsion slows the projectile on its approach trajectory [11]. In the present context, a significant concentration of positive holes in the vicinity of the back-scatter site is expected to significantly increase the back-scattered projectile energy, since a number of lattice sites would contribute in repelling the projectile. By this effect, the effective mass of the "target" would increase, leading in turn to a lower binary collision energy loss. In order to assess the overall effect on projectile energy, it is important to note that, for above-surface neutralization, mostly just one electron per halide site is expected to participate [11]. The positive charge building at the surface is thus spread over a number of iodine lattice sites, each separated by the 4.57 Å lattice constant. This charge distribution is further spread out due to diffusion of the created positive holes away from their original creation site. If the diffusional spreading occurs on time scales comparable or faster than the incident projectile–surface interaction time, then the overall effect of the positively charged hole distribution on the projectile energy will be small. This appears to be the case for the present measurements, as only a very small increase of scattered projectile energy is seen at the very lowest incident energies, which is consistent with projectile image-charge-interaction energy-gains seen e.g. for LiF [11,12].

Consistent with this negative result is our finding, shown in Fig. 4(b), that the ratio of scattered 2+/1+ peak areas does not increase with decreasing projectile incident energy, contrary to what would be expected in the presence of a significant positive charge build up at the surface, whose cumulative effect would be to progressively increase the turning point distance of the approaching projectile with decreasing energy, with consequent reduction of neutralization. Recent calculations involving normal impact of Ne^{10+} on LiF at energies comparable to those investigated in the present measurement, show no evidence of a "trampoline" effect as well [13]. It must be emphasized, however, that the insulators studied by Briand et al. [2] for which this effect was observed may have significantly lower hole diffusion rates and dielectric response than the CsI target of the present investigation or alkali halide crystals in general. It is therefore most likely premature to draw a general conclusion just on the basis of our present results.

4.2. Higher energy charge fraction measurements

Turning now to a discussion of the scattered charge fraction measurements in the energy range 3–32 keV shown in Figs. 5 and 6, because of the reasons already outlined in an earlier section, the

uncertainty of the data shown in both figures is significantly larger than was the case for the Au(1 1 0) target. Also, some of the features clearly evident in the various dependences of the scattered charge fractions seen for Au(1 1 0) are not as prominent in the CsI(1 0 0) results. For example, referring to Fig. 5, the sharp increase of the 2+ and higher scattered charge fractions with opening of the L-shell in the incident projectile (i.e. when going from charge state 8+ to 9+ and higher) is no longer as pronounced. This may be in part due to the fact that already for lower incident charge states the scattered charge states 2+ and higher show significantly higher fractions for CsI(1 0 0) than for Au(1 1 0). Interestingly, even for incident Ar^+ at 5 keV, for which the dominant scattered charge state is neutral, scattered charge states as high as 3+ were observed, indicating the presence of projectile ionization in addition to the dominant neutralization already at this relatively low energy. In general, the fractions of scattered charge states greater than 1+ exceed those observed for Au(1 1 0) by at least an order of magnitude both for the 5 keV measurements as function of incident charge, and for the fixed 11+ charge state measurements as function of initial projectile energy.

Also exhibiting markedly different behaviors are the 1+ and neutral scattered charge fractions. Whereas for the Au(1 1 0) target results, the scattered neutral fraction at fixed 5 keV energy stayed at or above 80% until the projectile L-shell opened, and then dropped to the 50% level when the L-shell opened, for the CsI(1 0 0) target, a more monotonic decrease of the scattered neutral fraction, from about 70% for incident 1+ to about 21% for incident 13+, is evident with increasing projectile charge. The scattered 1+ fraction climbs to a local maximum at roughly incident 8+ with increasing projectile charge, beyond which it falls again, as the higher scattered charge states, particularly 2+, become more prominent. As far as the energy dependences of the neutral and 1+ scattered charge fractions for incident 11+ are concerned, a striking difference is seen with the Au(1 1 0) results. While for Au(1 1 0), the neutral fraction dropped by more than a factor of 6 in the range 3–34 keV, the neutral fraction in the case of CsI(1 0 0) shows a slight rise from about 28% toward an intermediate maximum of about 40% at around 15 keV, and then a gradual decline to slightly above 30% at the highest investigated energy. Given the large uncertainties, one could as well call the neutral fraction independent of energy in this range.

In speculating about the possible reasons for this markedly different behavior, we consider the behavior of the Ar neutral level on the receding part of the trajectory, i.e. on the way out, where the scattered neutral charge state is most likely frozen in. In the case of the metal target, the Ar^0 level is promoted by the projectile image charge interaction, as a result of which resonant capture from the Au valence band [14] is always possible, as is Auger neutralization, since excitation of valence electrons into the conduction band is allowed in the metal case. In the insulator case, the neutral level is demoted, due to interaction with the positive hole left behind in the insulator surface. Target levels see a similar demotion. There is still some debate whether the initial and final state potential curves are parallel [15], or whether screening effects curtail this demotion of target levels at some point [16], resulting in a crossing of potential curves. In the present case, however, the Cs^+ valence band [17] lies slightly higher than the asymptotic Ar^0 level and no crossing is expected. It thus appears that at low energies only AN processes involving I lattice sites (i.e. the I^- valence band [17]) can contribute to Ar neutral formation in the ground state. Since scattering from both Cs and I lattice sites is included in the observed quasi-binary collisions considered here, the neutral fraction is thus reduced to about 50% at low energies, roughly consistent with the 70% neutral fraction seen for incident 1+. At progressively higher energy, broadening and overlap effects most likely bring RN processes involving the Cs lattice sites into play. These AN and RN processes very likely have opposite energy dependences, and we speculate that the combination of the two may result in the rather flat energy dependence observed experimentally.

So, as was the case in the grazing incidence geometry [18], the formation of scattered neutrals appears to be mainly determined by valence band interactions as the projectile recedes from the

surface. Not so clear is the extent to which the neutralization in the vicinity of the trajectory turning point leading up to this final step occurs just via interactions with target valence electrons as well. Calculations are obviously needed, e.g. based on suitably modified approaches of Díez Muiño et al. [19] or Burgdörfer et al. [20] to determine the relative contributions of the different dielectric response and atomic number for Au and CsI to the different highly charged-ion neutralization-responses of these two targets observed under quasi-binary collision conditions.

Acknowledgements

This research was sponsored in part by the Office of Fusion Energy Sciences, and by the Office of Basic Energy Sciences of the US Department of Energy under contract no. DE-AC05-0OR22725 with UT-Batelle, LLC. V.A.M. was appointed through the ORNL Postdoctoral Research Associates Program administered jointly by Oak Ridge Associated Universities and ORNL. J.M. gratefully acknowledges travel and subsistence support by the Deutscher Akademischer Austauschdienst (DAAD) during his stay at ORNL.

References

[1] F.W. Meyer et al., Phys. Scripta T 92 (2001) 182.
[2] J.-P. Briand et al., Phys. Rev. A 55 (1997) 2523;
J.-P. Briand et al., Rev. Sci. Inst. 71 (1999) 627.
[3] V.A. Morozov, F.W. Meyer, Phys. Rev. Lett. 86 (2001) 736;
V.A. Morozov, F.W. Meyer, Phys. Scripta T 92 (2001) 31.
[4] F.W. Meyer, V.A. Morozov, Nucl. Instr. and Meth. B 193 (2002) 530.
[5] F.W. Meyer, ECR-based atomic collision physics research at ORNLN MIRF, in: J. Gillaspy (Ed.), Trapping of Highly Charged Ions: Fundamentals and Applications, Nova Science Pub, New York, 2000, p. 117.
[6] F.W. Meyer, V.A. Morozov, Nucl. Instr. and Meth. B 157 (1999) 297.
[7] V.A. Morozov, F.W. Meyer, Rev. Sci. Instr. 70 (1999) 4515.
[8] F. Aumayr et al., Comments At. Mol. Phys. 34 (1999) 201.
[9] G. Hayderer et al., Phys. Rev. Lett. 86 (2001) 3530.
[10] W. Huang et al., Phys. Rev. A 56 (1997) 3777.
[11] Lotten Hägg et al., Phys. Rev. A 55 (1998) 2097.
[12] C. Auth et al., Phys. Rev. Lett. 74 (1995) 5244.
[13] L. Wirtz et al., Nucl. Instr. and Meth. B 182 (2001) 36.
[14] C.S. Fadley, D.A. Shirley, J. Res. NBS – A. Phys. Chem. 74A (1970) 543.
[15] C. Auth et al., Rev. A 57 (1998) 351.
[16] L. Wirtz et al., Surf. Sci. 451 (2000) 197.
[17] R.T. Poole et al., Phys. Rev. B 11 (1975) 5179.
[18] F.W. Meyer et al., Nucl. Instr. and Meth. B 125 (1997) 138.
[19] R. Díez Muiño et al., Phys. Rev. A 57 (1998) 1126.
[20] Joachim Burgdörfer et al., Nucl. Instr. and Meth. B 98 (1995) 415.